Available online at www.sciencedirect.com
SCIENCE DIRECT®
Physica E 25 (2005) 339–346
PHYSICA E
www.elsevier.com/locate/physe

Magneto conductance for tunnelling through double magnetic barriers

G. Papp[a,b,c], F.M. Peeters[b,*]

[a]Department of Theoretical Physics, University of Szeged, Aradi vtk. tere 1, H-6720 Szeged, Hungary
[b]Institute of Physics, University of West Hungary, Bajcsy Zs. út 5-7, H-9400 Sopron, Hungary
[c]Departement Fysica, Universiteit Antwerpen (Campus Drie Eiken), Universiteitsplein 1, B-2610 Antwerpen, Belgium

Received 27 May 2004; accepted 2 June 2004
Available online 29 September 2004

Abstract

The temperature-dependent magnetoresistance effect is investigated in a magnetically modulated two-dimensional (2D) electron gas (2DEG) which can be realized by depositing two parallel ferromagnets on top of a 2DEG electron gas. In the resonant tunnelling regime the transmission for the parallel and antiparallel magnetization configurations shows a quite distinct dependence on the longitudinal wave vector of the incident electrons. This leads to a very large magneto resistance ratio with a strong temperature dependence.

PACS: 73.40.−c; 75.75.+a; 72.20−i; 73.23.−b

Keywords: Giant magnetoresistance; Resonant tunnelling; Magnetic barriers

1. Introduction

Recently, there has been a lot of interest in the study of the electronic transport properties of semiconductor heterostructures in the presence of inhomogeneous magnetic fields. The experimental realization of magnetic dots and antidots, the patterning of ferromagnetic materials integrated with semiconductors allows one to create magnetic barriers or wells, periodic and quasi-periodic magnetic superlattices (For a recent review, see Ref. [1]). The magnetic barrier system [2] is very different from the well-known potential barrier because the electron tunnelling is now a two-dimensional (2D) problem. The transmission depends not only on the energy of the impeding electrons but also on the direction in which the electrons move towards the barrier.

*Corresponding author. Tel.: +32-3-820-2478; fax: +32-3-820-2245.
E-mail addresses: pgy@physx.u-szeged.hu (G. Papp), francois.peeters@ua.ac.be (F.M. Peeters).

1386-9477/$ - see front matter © 2004 Elsevier B.V. All rights reserved.
doi:10.1016/j.physe.2004.06.055

When not only the charge, but also the spin of the electrons is taken into account electronic transport can become spin-polarized [3–6]. Reports have explored the possibility of producing spin memory devices [7], and spin transistors [8], as well as exploiting the properties of spin coherence for quantum computation [9,10]. However, although there exists already a wealth of studies exploiting the electron spin as a degree of freedom in semiconductors, only limited interest was directed towards hybrid systems in which semiconductor and magnetic materials are combined [11]. Electron spin polarization in magnetically modulated quantum structures were investigated [12] with and without an external electric field and it was found, that the spin polarization strongly depends on the magnetic configuration, the applied bias, the incident electron energy, and the incident wave vector. Motivated by recent experimental results which demonstrated the existence of long relaxation times for spin-polarized distributions of carriers in the presence of transverse magnetic field [13] split-gate structures were proposed [14] as a tuneable spin filter.

The discovery of the so-called giant magnetoresistance (GMR) effect [15] has given rise to a tremendous economic impact on magnetic information storage [16]. Fueled by its fascinating practical applications such as ultra-sensitive magnetic field sensors, read heads, and random access memories, numerous theoretical and experimental studies are dealing with the GMR phenomenon (For a review, see Ref. [17]). The structures where GMR is observed generally consist of ferromagnetic layers separated by thin nonmagnetic layers. In such heterogeneous systems, GMR is characterized by a striking drop of the electric resistance when an external magnetic field switches the magnetizations of adjacent magnetic layers from an antiparallel (AP) alignment to a parallel (P) one. It is widely agreed that the spin-dependent scattering of electronic carriers results in different values (G_P and G_{AP}) of the conductance in the two configurations [18]. The spin-independent GMR effect was studied by Zhai et al. [19] in a magnetically modulated 2D electron gas (2DEG) which can be realized by depositing two parallel ferromagnets on top of the heterostructure. The authors found that transmission for parallel and antiparallel magnetization shows a quite distinct dependence on the longitudinal wave vector of the incident electrons, resulting in a tremendous zero temperature magnetoresistance (MR) ratio $(G_P - G_{AP})/G_{AP}$, which can be up to $10^6\%$ for realistic electron densities. The MR ratio can be further tuned by the inclusion of an electric barrier.

In the present paper, we study the effect of temperature on the GMR of Ref. [19] and include the spin of the electrons. The magnetic barriers are created by depositing on top of a heterostructure two parallel metallic ferromagnetic stripes with widths d and magnetizations along the x-axis. When a magnetic field is directed parallel to the 2DEG the magnetic material becomes magnetized parallel to the 2D plane which leads to fringing fields near the edge of the magnetic material having a non-homogeneous magnetic field component perpendicular to the 2DEG (as e.g. was demonstrated experimentally in Ref. [20]). The fringe field of each ferromagnet induces a positive B_z underneath one edge of the stripe and a negative B_z underneath the other edge. A suitable external magnetic field can change the relative orientation of the two magnetizations, which is antiparallel at zero field. For small distances between the 2DEG and the ferromagnets, the magnetic barrier can be approximated by delta functions, i.e.

$$B_z(x) = Bl_B\Big\{\mathrm{sign}(x)\Big[\delta\Big(|x| - \frac{w}{2}\Big) - \delta\Big(|x| - d - \frac{w}{2}\Big)\Big]p_s(x)\Big\}.$$

Here, B gives the strength of the magnetic field, $l_B = \sqrt{hc/eB_0}$ is the magnetic length for an estimated magnetic field B_0, $\mathrm{sign}(x)$ is the sign function, $p_s(x)$ represents the magnetization configuration ($p_s(x) = +1$ for P and $p_s(x) = -\mathrm{sign}(x)$ for AP), d is the width and w is the distance between the two stripes of the structure along the current direction (x). The model magnetic field for parallel (b) and anti-parallel (a) configurations are schematically depicted in Fig. 1.

The present paper is organised as follows. In Section 2 we derive the Schrödinger equation of our system, and show how it transforms to an

effective 1D problem. The numerical results and our discussions are presented in Section 3 and the conclusions are given in Section 4.

2. Theoretical model

We consider a 2DEG moving in the (x, y)-plane in the presence of the inhomogeneous magnetic field profiles $\mathbf{B} = B_z(x)\mathbf{e}_z$ depicted in Figs. 1(a) and (b). The δ-function magnetic field profile is a result of the fringe fields of the ferromagnet and we assume that the effect of the parallel magnetic field component on the electron can be neglected. The Hamiltonian describing such a system, in the single particle effective mass approximation, is

$$H = \frac{p_x^2}{2m^*} + \frac{(p_y + e/cA_y(x))^2}{2m^*} + \frac{eg^*}{2m_0}\frac{\sigma\hbar}{2c}B_z(x), \quad (1)$$

where m^* is the effective mass, and m_0 the free electron mass, (p_x, p_y) is the electron momentum, g^* is the effective Landé-factor of the electron in the 2DEG. $\sigma = +1/-1$ for spin up/down electrons, and the magnetic vector potential of our magnetic barriers will be expressed in the Landau gauge $(0, A_y(x), 0)$. As the system is translational invariant along the y-direction the solution of the stationary Schrödinger equation $H\Psi(x, y) = E\Psi(x, y)$ can be written as a product $\Psi(x, y) = e^{ik_y y}\psi(x)$, where $\hbar k_y$ is the expectation value of the momentum p_y in the y-direction. The wave function $\psi(x)$ satisfies the following one-dimensional (1D) Schrödinger equation:

$$\left[\frac{\mathrm{d}^2}{\mathrm{d}x^2} - \left(k_y + \frac{e}{c\hbar}A_y(x)\right)^2 + \frac{2m^*}{\hbar^2}\left\{E - \frac{eg^*}{2m_0}\frac{\sigma\hbar}{2c}B_z(x)\right\}\right]\psi(x) = 0. \quad (2)$$

If we introduce the following characteristic parameters [2]: $\omega_c = eB_0/m^*c$ with B_0 some typical magnetic field, and l_B the corresponding magnetic length then, the Schrödinger equation becomes

$$\left[\frac{\mathrm{d}^2}{\mathrm{d}x^2} + 2(E - V(x, k_y))\right]\psi(x) = 0, \quad (3)$$

where all quantities are expressed in dimensionless units: $x \to l_B x$, $E \to \hbar\omega_c E$ and

$$V(x, k_y) = \frac{(k_y + A_y(x))^2}{2} + \frac{g^* m^* \sigma B_z(x)}{4m_0}, \quad (4)$$

with $A_y \to B_0 l_B A_y$, $B_z(x) \to B_0 B_z(x)$ and $k_y \to k_y/l_B$. The problem is now reduced to a 1D tunnelling problem. The 1D potential $V(x, k_y)$ depends on the wave vector k_y, the arrangement of the magnetic stripes, and also on the interaction between the non-homogeneous magnetic field and the electron spin.

The potential given by Eq. (4) can, for the magnetic field configurations of Figs. 1(a) and (b) be written as follows:

$$V(x, k_y) = \begin{cases} k_y^2/2, & -\infty < x < 0, \\ \dfrac{(B + k_y)^2}{2} + \dfrac{g^* m^* \sigma B}{2m_0}\delta(x), & x = 0, \\ \dfrac{(B + k_y)^2}{2}, & 0 < x < x_1, \\ \dfrac{(B + k_y)^2}{2} - \dfrac{g^* m^* \sigma B}{2m_0}\delta(x - x_1), & x = x_1, \\ \dfrac{k_y^2}{2}, & x_1 < x < x_2, \\ \dfrac{(p_s B + k_y)^2}{2} + \dfrac{g^* m^* \sigma B}{2m_0} p_s \delta(x - x_2), & x = x_2, \\ \dfrac{(p_s B + k_y)^2}{2}, & x_2 < x < x_3, \\ \dfrac{(p_s B + k_y)^2}{2} - \dfrac{g^* m^* \sigma B}{2m_0} p_s \delta(x - x_3), & x = x_3, \\ \dfrac{k_y^2}{2}, & L < x < \infty, \end{cases} \quad (5)$$

where $x_1 = d$, $x_2 = d + w$ and $x_3 = 2d + w = L$. Consider now electron tunnelling through this potential. The initial free-electron wave function for $x < 0$ is $\psi_i(x) = A_+ \exp(\mathrm{i}k_i x) + A_- \exp(-\mathrm{i}k_i x)$ and the final one for $x > L$ is $\psi_f(x) = B_+ \exp[\mathrm{i}k_f(x - L)] + B_- \exp[-\mathrm{i}k_f(x - L)]$ where $k_i = k_f = \sqrt{2E - k_y^2}$ is the x-component of the

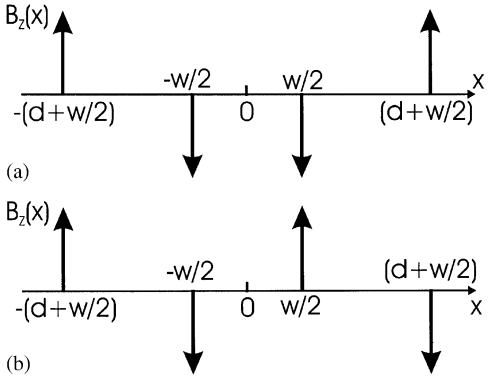

Fig. 1. Theoretical model for the magnetic field profile for the anti-parallel (a) and parallel (b) configurations of the two magnetic stripes which are placed on top of the heterostructure.

electron wave vector on the corresponding sides of the structure. Within the active range, on the right-hand side of the first magnetic peak $(0<x<x_1)$ we have $\psi_1(x) = A_1 \exp(ik_1x) + B_1 \exp(-ik_1x)$ and on the left-hand side of it $(x_2>x>x_1)\,\psi_2(x) = A_2 \exp[ik_2(x-x_1)] + B_2 \exp[-ik_2(x-x_1)]$, while for $(x_2<x<x_3)\,\psi_3(x) = A_3 \exp[ik_3(x-x_2)] + B_3 \exp[-ik_3(x-x_2)]$ where $k_1 = \sqrt{2E-(k_y+B)^2}$, $k_2 = \sqrt{2E-k_y^2}$ and $k_3 = \sqrt{2E-(k_y+p_sB)^2}$, are the x-components of the electron wavevector. The δ-functions in the effective potential introduces discontinuity in the first derivative of the wave function. Matching the wave functions and their derivatives within the potential barrier and at the edges of the barrier the coefficients of the final state can be obtained from the coefficients of the initial state with the help of the matrix equation

$$\begin{pmatrix} B_+ \\ B_- \end{pmatrix} = M \begin{pmatrix} A_+ \\ A_- \end{pmatrix}, \tag{6}$$

where M is the so-called transfer matrix

$$M = \frac{1}{2}\begin{pmatrix} 1 & -\dfrac{i}{k_f} \\ 1 & \dfrac{i}{k_f} \end{pmatrix} S \begin{pmatrix} 1 & 1 \\ ik_i & -ik_i \end{pmatrix} \tag{7}$$

and $S = S_3S_2S_1$ is a 2×2 matrix, where the S_j for $j=2$ is given by

$$S_2 = \begin{pmatrix} \cos(k_2w) & \dfrac{1}{k_2}\sin(k_2w) \\ -k_2\sin(k_2w) & \cos(k_2w) \end{pmatrix}$$

and S_j for $j=1$ or 3 is

$$S_j = \begin{pmatrix} \cos(k_jd) - \dfrac{c}{k_j}\sin(k_jd) & \dfrac{1}{k_j}\sin(k_jd) \\ -\left(k_j + \dfrac{c^2}{k_j}\right)\sin(k_jd) & \cos(k_jd) + \dfrac{c}{k_j}\sin(k_jd) \end{pmatrix}$$

with $c = -g^*Bm^*\sigma/2m_0$ for $j=1$ and with $c = g^*Bm^*\sigma/2m_0p_s$ for $j=3$.

From the transfer matrix the spin-dependent transmission probability through the potential system $T_\sigma(E,k_y)$ is obtained

$$T_\sigma(E,k_y) = \frac{k_i}{k_f}\frac{1}{|M_{22}|^2}. \tag{8}$$

The electron spin polarization is defined by

$$P(E,k_y) = \frac{T_+(E,k_y) - T_-(E,k_y)}{T_+(E,k_y) + T_-(E,k_y)}. \tag{9}$$

Following Ref. [2] we calculate the electric current through such a structure, in the ballistic regime. The conductance G is obtained as the electron flow averaged over half the Fermi surface [21]

$$G = 2G_0 \sum_{\sigma=-,+} \int_{-\pi/2}^{\pi/2} T_\sigma(E_F, \sqrt{2E_F}\sin\phi, U) \times \cos\phi\, d\phi, \tag{10}$$

where ϕ is the angle of incidence relative to the x-direction, $G_0 = e^2m^*v_FL_y/h^2$ [22],[1] where L_y is the length of the structure in the y-direction and v_F the Fermi velocity.

3. Results and discussions

In our numerical calculation materials parameters were taken for the GaAs and InAs system where the electron effective masses are

[1] The expression of G_0 in Eq. (6) of Ref. [2(b)] should be divided by $2\pi^2$.

$m^*_{GaAs} = 0.067m_0$ and $m^*_{InAs} = 0.024m_0$ and the effective Landé-factors $g^*_{GaAs} = 0.44$ and $g^*_{InAs} = 15$, respectively. We take typically for GaAs $n_e \approx 10^{11}\,cm^{-2}$ which gives $E_F = 3.55\,meV$ and for InAs $n_e \approx 10^{12}\,cm^{-2}$ $E_F = 99.1\,meV$ and use $B_0 = 0.1\,T$ which is a realistic value. This leads to the units $l_B = 813\,\text{Å}$, and $E_0 = \hbar\omega_c = 0.17\,meV$ and $E_0 = 0.47\,meV$ for GaAs and InAs, respectively.

Fig. 2 presents the transmissions for P alignment when the spin-magnetic field interaction is neglected for (a) $0 \leqslant k_y \leqslant 2$ and (b) $-2 \leqslant k_y \leqslant 0$ where curves are shown in steps of $\Delta k_y = 0.5$. The magnetic barriers, for values of k_y which are larger than $-B/2$, behave as quantum-barriers and the middle region between the two ferromagnets acts as a quantum well, and consequently the transmission behaviour is similar to resonant tunnelling through a double-barrier quantum-well structure, as is clearly seen in Fig. 2 where the transmission probability is shown for $B = 5$, $d = 1$ and $w = 3$. For both two k_y intervals there exist several delta-function-shaped resonant peaks with value unity. The magnetic barriers, for values of k_y which are less than $-B/2$, behave as quantum-wells. Such alignment of the magnetic field barriers does not lead to any spin polarization. Of course spin-orbit interaction (which is neglected in the present paper) will change the transmission as compared to the zero-spin case.

Fig. 3(a) shows the transmission probability of the electron as a function of energy without considering the spin for the AP alignment for $0 \leqslant k_y \leqslant 2$ with $\Delta k_y = 0.5$ between subsequent curves. When electron spin is included we obtain in Fig. 3(b) the spin polarization (see Eq. (9)) with $k_y = 0, 1, 2$ for InAs [23]. The potential has for the AP alignment an even symmetry with respect to $k_y \to -k_y$. As we know, for particles traversing a potential in opposite direction the transmission is always equal. Therefore, such symmetry results in the invariance of the transmission with respect to the replacement $k_y \to -k_y$. The potential, for values of k_y which are less than $B/2$, behave as an asymmetric double-barrier quantum-well, so for small k_y values one can observe sharp resonances where the transmission probabilities are less than unity. The potential, for values of k_y which are larger than $B/2$, consists of a barrier and a well. When the spin-magnetic field interaction is included the transmission probability is altered for all values of the energy, especially at the resonant energies. The resonant peak shifts to higher energy for the spin-down electron, and to lower energy for the spin-up electron but this shift is non symmetric. The polarization varies fast with the incident electron energy (see Fig. 3(b)). The position of the sign changes does not coincide with the resonant positions in the transmission (see Fig. 3(a)) in the absence of spin. However for GaAs the above two energy values are very close, but for InAs they are completely different due to

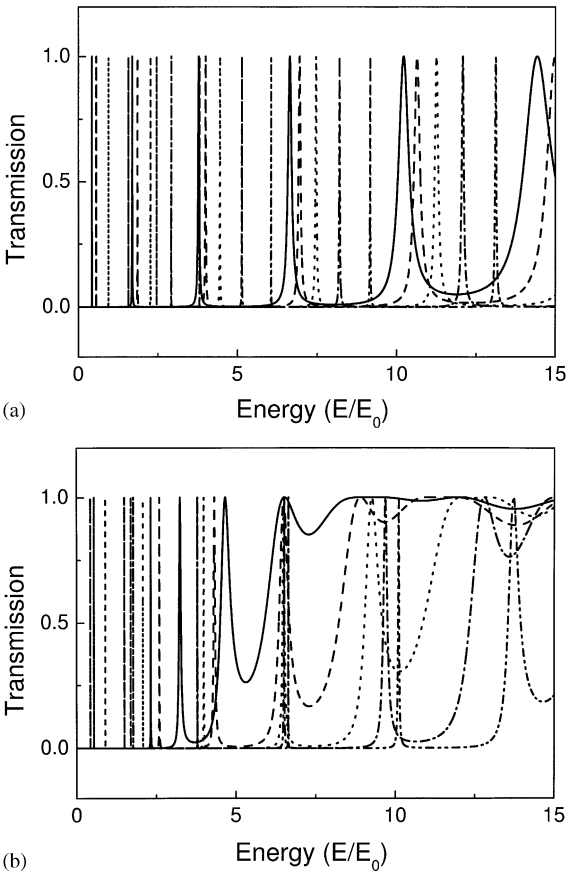

Fig. 2. The transmission probability for spinless electrons tunnelling through magnetic barriers with parallel magnetizations as a function of energy for (a) $0 \leqslant k_y \leqslant 2$ and (b) $-2 \leqslant k_y \leqslant 0$. Subsequent curves are for steps with $\Delta k_y = 0.5$. The $k_y = 0$ value corresponds to the solid line. The magnetic structure parameters are $B = 5.0$, $d = 1$, and $w = 3$.

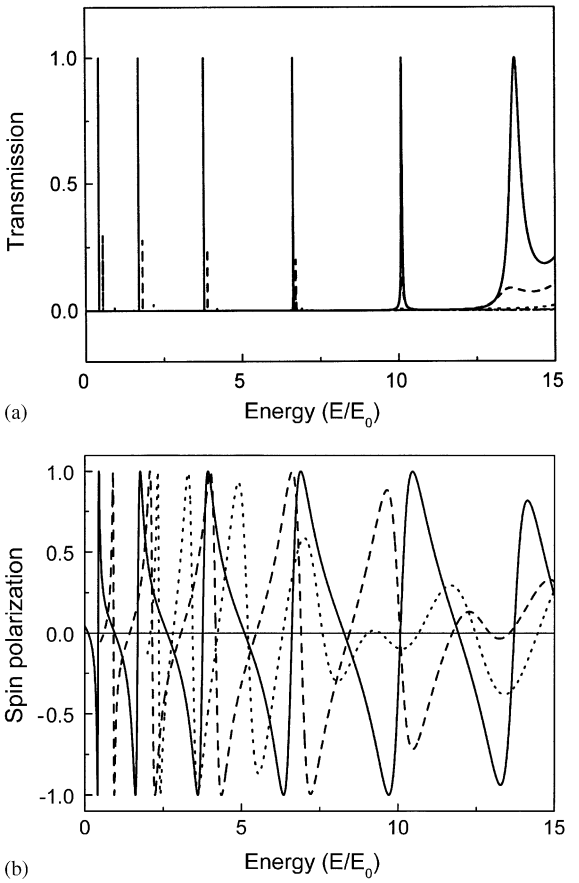

Fig. 3. The transmission probability for spinless electrons as a function of energy in the case of AP alignment for different values of $k_y = 0, 1, 2$ (solid, dashed, dotted curve, respectively). The electron spin-polarization when the electron spin is included with $k_y = 0, 1, 2$ for InAs (b). The solid curves in (a) and (b) are for $k_y = 0$.

the more pronounced asymmetric shift in the transmission. The polarization of the transmitted electron beams can reach $\sim 100\%$ at resonance even in the case of incomplete transmission. The reason is that T_- almost disappears for those energies where T_+ is in resonance. The resonance peaks are extremely sharp (see Fig. 3(a)). For higher energy the rate of spin polarization decreases. The resonant peaks for both spin-up and spin-down electrons shift to lower energy by increasing the separation and/or decreasing the magnetic barrier height. But this shift is different for spin-up and spin-down electrons. The electronic spin and the local magnetic field interaction depends on the quantity $g^*Bm^*/2m_0$. For $B = 5$ the value of the latter is 0.0737 for GaAs and 0.9 for InAs and therefore will neglect the spin-dependent part in the subsequent discussion.Having seen the transmission and polarization results, one may wonder to what extent their structure is reflected in measurable quantities, which often involve some kind of averaging. In Fig. 4 we show the conductance vs. Fermi energy, as given by Eq. (10). For comparison, we drew the curve of P and AP conductance normalized with respect to $2G_0$ (solid). To generalize our results to nonzero temperature we have to replace any function of $G(E_F)$ which depends on the Fermi energy E_F by the corresponding average over the derivative of the Fermi function:

$$G(\mu) = \int \mathrm{d}\varepsilon G(\varepsilon)\left(-\frac{\partial f_0}{\partial \varepsilon}\right),$$

where

$$f_0 = \{\exp[(\varepsilon - \mu)/k_B T] + 1\}^{-1}.$$

In Fig. 4 we show the conductance for $T = 0.2\,\mathrm{K}$ (dashed) and $T = 1\,\mathrm{K}$ (dotted). In the low-energy region, for both P and AP alignments, the transmission peaks are extremely sharp and the conductance is almost zero. Notice the large difference in conductance between the P and AP alignments. G_P exhibits an initial rapid increase (this is absent in G_{AP}) which for $E_F/E_0 \geqslant 5$ becomes almost linear in the Fermi energy. In addition, the G_P curve has a striking conductance peak with a large peak-to-valley ratio (i.e. for $E_F/E_0 \approx 6.5$) as well as several small peaks. The reason is, for electrons with negative k_y value the resonant tunnelling interval is shorter (see Fig. 2(b)) and these electrons together with the resonant tunnelling electrons incident with positive k_y component lead to the peaks in the conductance. The thermal fluctuations destroy the sharp peaks in the conductance and for $T \geqslant 1\,\mathrm{K}$ they are all smoothed out. Fig. 5 shows the magneto resistance ratio for $T = 0\,\mathrm{K}$ (solid) and $T = 0.2\,\mathrm{K}$ (dashed) and in the inset for $T = 1\,\mathrm{K}$ (solid curve) and $T = 10\,\mathrm{K}$ (dashed curve, which is referred to the right axis). The giant magnetic resistance is due to the definition of MR, since it

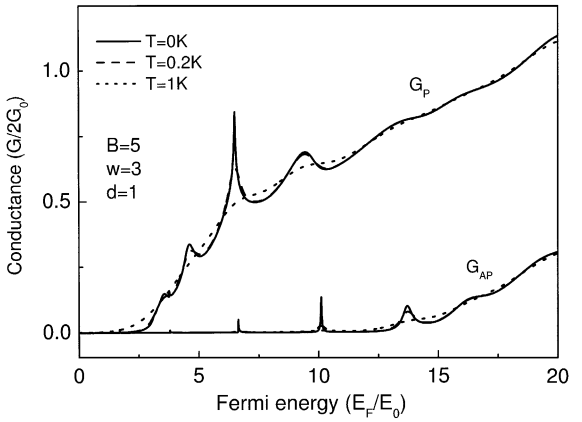

Fig. 4. The conductance of electrons as a function of the Fermi energy for both P and AP alignments for different temperature: $T = 0\,\mathrm{K}$ (solid), $T = 0.2\,\mathrm{K}$ (dashed) and $T = 1\,\mathrm{K}$ (dotted). The magnetic structure parameters are the same as those in Fig. 2.

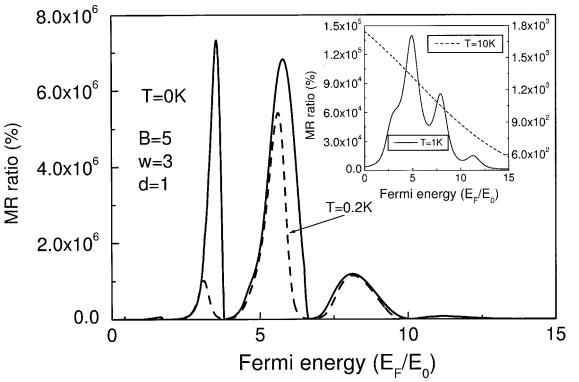

Fig. 5. The MR ratio vs. the Fermi energy for different temperature: $T = 0\,\mathrm{K}$ (solid), $T = 0.2\,\mathrm{K}$ (dashed). In the inset the MR ratio is shown for $T = 1\,\mathrm{K}$ (solid) and $T = 10\,\mathrm{K}$ (dashed and referred to the right axis). The magnetic structure parameters are the same as those in Fig. 2.

contains in its denominator G_{AP} which is much smaller than G_{P}. The effect of temperature is: (i) to shift the peaks in the MR ratio to lower Fermi energy, and (ii) to broaden them and eventually for $T \gg 1\,\mathrm{K}$ those peaks are completely disappeared. To see the definition dependence of the huge MR better, we calculated the modified magneto resistance (MMR) ratio defined by $(G_{\mathrm{P}} - G_{\mathrm{AP}})/(G_{\mathrm{P}} + G_{\mathrm{AP}})$, which we show in Fig. 6. For low Fermi energy the particular features of the behaviour of G_{P} and G_{AP} are clearly visible. The deep valleys due to the resonances are removed by temperature. Potential barriers can be used [19] to shift the MR peaks towards higher Fermi energy. Notice that already for $T = 1\,\mathrm{K}$ (see inset of Fig. 6) any device significant difference between the P and AP alignment have almost completely disappeared.

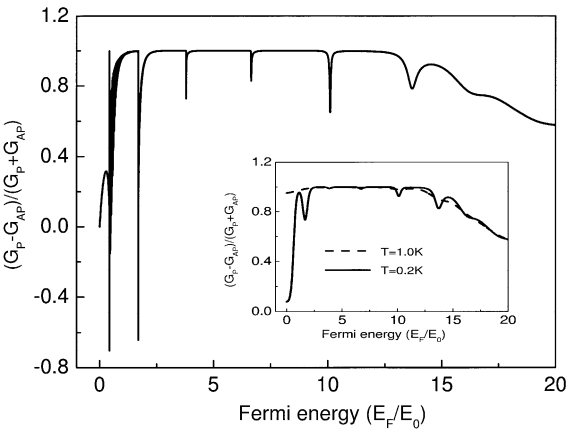

Fig. 6. The MMR vs. the Fermi energy for $T = 0\,\mathrm{K}$. In the inset, the MMR vs. Fermi energy is shown for $T = 0.2\,\mathrm{K}$ (solid) and for $T = 1\,\mathrm{K}$ (dashed). The magnetic structure parameters are the same as those in Fig. 2.

4. Conclusions

Two parallel ferromagnetic stripes with magnetization along the current direction, deposited on top of a two dimensional electron gas, create magnetic barriers for motion of the electrons in the plane. Resonance tunnelling of two-dimensional electrons through such magnetic barriers leads to a giant magnetic resistance effect. The latter decreased strongly with temperature. The peaks of the MR ratio are shifted to lower Fermi energy and disappear with increasing temperature. Furthermore, in practical devices not only in the MR ratio important but also the MMR ratio, i.e. $(G_{\mathrm{P}} - G_{\mathrm{AP}})/(G_{\mathrm{P}} + G_{\mathrm{AP}})$. We found that the latter reduces practically to one for $T > 1\,\mathrm{K}$ and decreases to zero at large Fermi energy.

Acknowledgements

Part of this work was supported by the Flemish Science Foundation (FWO-VI), the 'Inter-University Poles of Attraction Program-Belgian State, Prime Minister's Office-Federal Office for Scientific Technical and Cultural Affairs' (IUAP), the 'Onderzoeksraad van de Universiteit Antwerpen' (GOA), and the Flemish-Hungarian exchange programme.

References

[1] F.M. Peeters, J. De Boeck, in: H.S. Nalwa (Ed.), Handbook of Nanostructured Materials and Nanotechnology, vol. 3, Academic Press, New York, 1999, p. 345.
[2] [a] F.M. Peeters, A. Matulis, Phys. Rev. B 48 (1993) 15166;
[b] A. Matulis, F.M. Peeters, P. Vasilopoulos, Phys. Rev. Lett. 72 (1994) 1518(b).
[3] A. Voskoboynikov, S.S. Liu, C.P. Lee, Phys. Rev. B 59 (1999) 12514;
A. Voskoboynikov, S.S. Liu, C.P. Lee, Phys. Rev. B 58 (1998) 15397;
M. Sharma, S.X. Wang, J.H. Nickel, Phys. Rev. Lett. 82 (1999) 616.
[4] P. Pfeffer, W. Zawadzki, Phys. Rev. B 59 (1999) R5312.
[5] E.A. de Andrada e Silva, G.C. La Rocca, Phys. Rev. B 59 (1999) R15583.
[6] L. Viña, J. Phys.: Condens. Matter 11 (1999) 5929.
[7] J.M. Kikkawa, I.P. Smorchkova, N. Samarth, D.D. Awschalom, Science 277 (1997) 1284.
[8] D.J. Monsma, R. Vlutters, J.C. Lodder, Science 281 (1998) 407.
[9] D.P. DiVincenzo, Science 270 (1995) 255;
D. Loss, D.P. DiVincenzo, Phys. Rev. A 57 (1998) 120;
G. Burkard, D. Loss, D.P. DiVincenzo, Phys. Rev. B 59 (1998) 2070.
[10] B.E. Kane, Nature (London) 393 (1998) 133.
[11] V.N. Dobrovolsky, D.I. Sheka, B.V. Chernyachuk, Surf. Sci. 397 (1998) 333.
[12] Y. Guo, B.L. Gu, Z. Zheng, J.Z. Yu, Y. Kawazoe, Phys. Rev. B 62 (2000) 2635;
Y. Guo, F. Zhai, B.L. Gu, Y. Kawazoe, Phys. Rev. B 66 (2002) 045312;
G. Papp, F.M. Peeters, Appl. Phys. Lett. 78 (2001) 2184;
G. Papp, F.M. Peeters, Appl. Phys. Lett. 79 (2001) 3198;
H.Z. Xu, Y. Okada, Appl. Phys. Lett. 79 (2001) 3119.
[13] J.A. Gupta, D.D. Awschalom, X. Peng, A.P. Alivisatos, Phys. Rev. B 59 (1999) R10421.
[14] M.J. Gilbert, J.P. Bird, Appl. Phys. Lett. 77 (2000) 1050.
[15] M.N. Baibich, J.M. Broto, A. Fert, F. Nguyen Van Dau, F. Petroff, P. Etienne, G. Creuzet, A. Friederich, J. Chazelas, Phys. Rev. Lett. 61 (1988) 2472.
[16] G.A. Prinz, Science 282 (1998) 1660.
[17] P.M. Levy, Solid State Phys. 47 (1994) 367;
M.A.M. Gijs, G.E.W. Bauer, Adv. Phys. 46 (1997) 285;
J-Ph. AnSermet, J. Phys.: Condens. Matter 10 (1998) 6027.
[18] K.M. Schep, P.J. Kelly, G.E.W. Bauer, Phys. Rev. B 57 (1998) 8907.
[19] F. Zhai, Y. Guo, B-L. Gu, Phys. Rev. B 66 (2002) 125305.
[20] V. Kubrak, F. Rahman, B.L. Gallagher, P.C. Main, M. Henini, C.H. Marrows, M.A. Howson, Appl. Phys. Lett. 74 (1999) 2507;
T. Vančura, T. Ihn, S. Broderick, K. Ensslin, W. Wegscheider, M. Bichler, Phys. Rev. B 62 (2000) 5074.
[21] M. Büttiker, Phys. Rev. Lett. 59 (1986) 1761.
[22] A. Matulis, F.M. Peeters, Phys. Rev. B 62 (2000) 91.
[23] H.Z. Xu, Z. Shi, Appl. Phys. Lett. 81 (2002) 691;
G. Papp, F.M. Peeters, Appl. Phys. Lett. 82 (2003) 3570.